Novel gas target for laser wakefield accelerators ⊘

C. Aniculaesei; Hyung Taek Kim (ID) ; Byung Ju Yoo; Kyung Hwan Oh; Chang Hee Nam (ID)

Check for updates

View Online

Export Citation

Novel gas target for laser wakefield accelerators

C. Aniculaesei,[1,a)] Hyung Taek Kim,[1,2,a)] Byung Ju Yoo,[1] Kyung Hwan Oh,[1] and Chang Hee Nam[1,3]

[1]*Center for Relativistic Laser Science, Institute for Basic Science (IBS), Gwangju 61005, South Korea*
[2]*Advanced Photonics Research Institute, Gwangju Institute of Science and Technology (GIST), Gwangju 61005, South Korea*
[3]*Department of Physics and Photon Science, GIST, Gwangju 61005, South Korea*

A novel gas target for interactions between high power lasers and gaseous medium, especially for laser wakefield accelerators, has been designed, manufactured, and characterized. The gas target has been designed to provide a uniform density profile along the central gas cell axis by combining a gas cell and slit nozzle. The gas density has been tuned from $\sim 10^{17}$ atoms/cm^3 to $\sim 10^{19}$ atoms/cm^3 and the gas target length can be varied from 0 to 10 cm; both changes can be made simultaneously while keeping the uniform gas profile. The gas density profile inside the gas cell has been measured using interferometry and validated using computational fluid dynamics. *Published by AIP Publishing.*
https://doi.org/10.1063/1.4993269

I. INTRODUCTION

The laser wakefield acceleration (LWFA)[1] in the bubble/blowout regime uses nonlinear plasma waves,[2] created by the interaction between a high power laser pulse and an underdense plasma medium to trap and accelerate plasma electrons towards relativistic velocities. One of the important issues in LWFA research is the control of accelerated electron energy. The energy of the accelerated electrons can be estimated by a formula,[3] $\Delta E \, [\text{GeV}] \approx 1.7 \left(\frac{P[\text{TW}]}{100}\right)^{1/3} \left(\frac{10^{18}}{n_p(\text{cm}^{-3})}\right)^{2/3} \left(\frac{0.8}{\lambda_0(\mu\text{m})}\right)^{4/3}$, where ΔE is the energy gained by the electrons, P is the laser power, n_p is the plasma density, and λ_0 is the laser wavelength. In general, the maximum achievable electron energy increases as the acceleration length and the laser power increase and/or plasma density is lowered. Thus, a laser pulse below 100-TW (Tera Watt) peak power can produce a few 100 MeV's electron beams in millimeters long gas targets,[4] while a PW (Peta Watt) laser pulse[5,6] can generate several GeV electron beams with centimeters long gas targets.[7–9] As the laser power increases rapidly to multi-PW level, a long and uniform gas medium over 10-cm length is required to obtain an electron beam over 10 GeV energy. However, conventional supersonic gas nozzles,[10] conical[11] or slit type,[12] cannot generate such a long and uniform density profile[13] due to a high gas load and non-uniform gas expansion.

A long gas medium can be produced by using gas cells,[14] which are small chambers filled with gas and having two apertures: one to let the laser enter the interaction region and one to let the accelerated electrons exit the gas cell. Some gas cells can have a variable length from 0 up to a few centimeters.[15] For the generation of a 10-GeV electron beam with multi-PW lasers, a gas medium should be designed to have a uniform, length tunable up to tens of centimeters long, density around 10^{17} atoms/cm^3 and relatively big entrance diameter to let the laser pass through the gas medium. Usual gas cells are not easy

to be designed to fulfill these requirements simultaneously due to the formation of a gas density spike at the gas inlet, particularly when low gas density is required in the cell. As an example, we perform a computational fluid dynamics (CFD) simulation for a typical gas cell of 2 cm × 2 cm × 3 cm (height × width × length) with a 2 mm inlet diameter and 2 mm outlets diameter, as shown in Fig. 1. The gas density spike is clearly visible around the inlet, and the density difference between the spike and the uniform region is more than 30% in this case. The gas density spike issue can be mitigated by reducing the backing pressure, reducing the inlet size, decreasing the outlet diameter, or decreasing the gas cell length, but cannot be eliminated in a typical gas cell while trying to fulfill all the above mentioned requirements. The reduction of inlet pressure and inlet size subsequently limits the achievable density range while the reduction of the outlet diameter can pose serious problems when laser pointing is not stable. Thus, taking into consideration all the requirements, the typical gas cell is not suitable for LWFA with PW lasers and a new type of gas target has to be designed.

In the present work, we report a new type of gas medium suitable for 10 GeV electron acceleration driven by multi-PW laser pulses[22] by combining elements from a typical gas cell and a slit nozzle to provide a gas target with a uniform gas density profile whose length and density are tunable. To avoid unnecessary repetition or confusion, in this article we call "*SlitCell*" the novel gas target. We have performed a series of CFD simulations to verify if the concept of *SlitCell* is realizable. Based on CFD simulation results, we have designed and manufactured a new type of gas target having variable length from 0 to 10 cm. The density distribution inside the gas target has been characterized through interferometry.

II. DESIGN, SIMULATION, AND CHARACTERIZATION

A. *SlitCell* design

A suitable gas target for LWFA should have a tunable density and length, with a uniform density profile. To fulfill

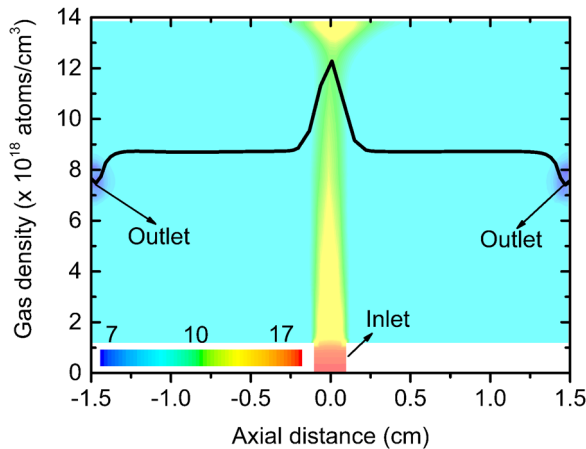a)htkim@gist.ac.kr and CA182@ibs.re.kr

FIG. 1. Simulated 2D contour density of a cross section through the center of a 3D gas cell (background) and the gas density taken along a line through the center (foreground). The gas cell has 2 mm gas inlet, 2 cm height, 2 cm width, and 3 cm length and the working gas is He at a pressure of 1 bar. The gas density spike is present around the gas inlet. The colormap is in logarithmic scale in units of 10^{18} atoms/cm^{-3}.

these criteria, especially for long acceleration lengths, we have decided to design a shaped inlet for the gas cells to neutralize the gas density spike mentioned in Sec. I and obtain a uniform gas density for various ranges of gas density and medium lengths. After comprehensive simulations using a commercial CFD code (ANSYS Fluent), we have modified the inlet of gas cell to have a slit nozzle shape rather than the usual cylindrical inlet shape. As shown in Fig. 2, the slit nozzle part has a cylindrical gas inlet with a diameter of 0.1 mm and a length of 2-mm, and a rectangular outlet at 20 mm above the inlet with the dimension of $20 \times 20 \times 90$ mm. The gas inlet is fed with gas through a 2 mm diameter quick-connect type connector shown in Figs. 2 and 3. The slit nozzle outlet fits exactly one side of the gas cell, as shown in Fig. 3, and the gas flows through this surface to fill the gas cell section. The gas cell has five surfaces and is placed on top of the slit nozzle part to contain the gas medium; two gas outlets are placed at front and back sides of the cell, and three optical windows are mounted at two sides and top surface. The windows permit optical access to the interior of the gas cell for probing the LWFA process and monitoring the visible radiation emitted by plasma. The two ends of the gas cell have two 1.4 mm diameter outlets,

FIG. 3. Photograph of the 10 cm length tunable *SlitCell*.

one outlet placed at the front and the other outlet placed on a movable rectangular insert part. The movable part is motorized and controlled via a computer to change the effective distance between the two outlets between 0 and 100 mm. The "*Slit-Cell*" design has been characterized using computational fluid dynamics simulations which are presented in Sec. II B.

B. CFD simulations for SlitCell design

We have performed CFD simulations using the ANSYS Fluent[16] that can solve the Navier-Stokes equations[17,18] on a 3-dimensional mesh containing hexahedral cells with various volumes between 10^{-12} m^3 and 10^{-16} m^3. On average, each mesh contained at least 3×10^6 cells. A turbulent model, the k-ω shear stress transport model,[19] has been used with double accuracy. The gas inlet has been chosen as the pressure inlet which feeds He gas of various pressures at 300-K temperature. The outlets are chosen as pressure outlets at 10^{-3} mbar pressure and the walls are considered adiabatic. Also mesh-independence tests have been run to ensure that the simulation result does not depend on the mesh size.

The ANSYS Fluent simulations have been run with two different objectives:

- To establish the most suitable geometry, dimensions, and shape for the final design of the *SlitCell* to provide the desired density profile.
- To predict the density profile of the *SlitCell* for different experimental conditions such as inlet pressures or medium lengths.
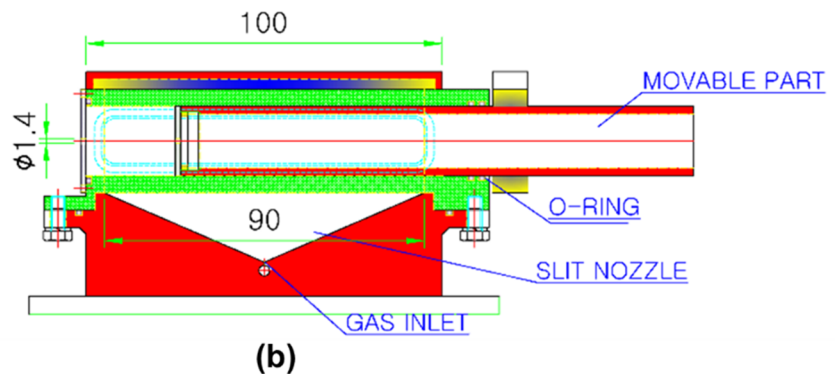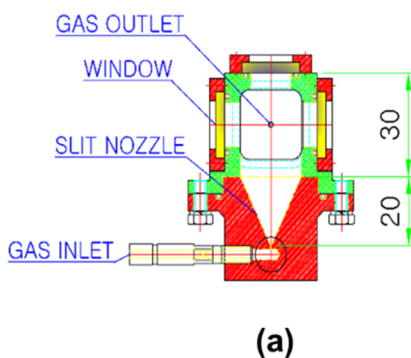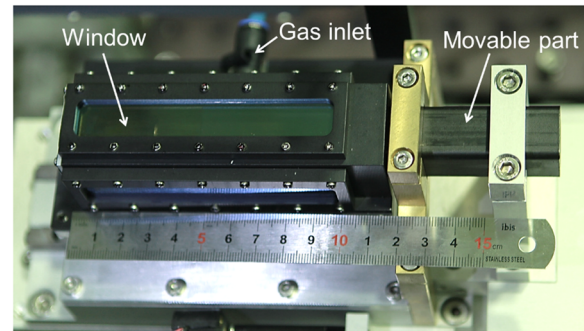

FIG. 2. Drawing of the *SlitCell* for (a) the front view and (b) the side view. The movable part is mounted on a translation stage to vary the distance between two outlets. The *SlitCell* is equipped with two lateral windows and one top fused silica window for monitoring the LWFA process.
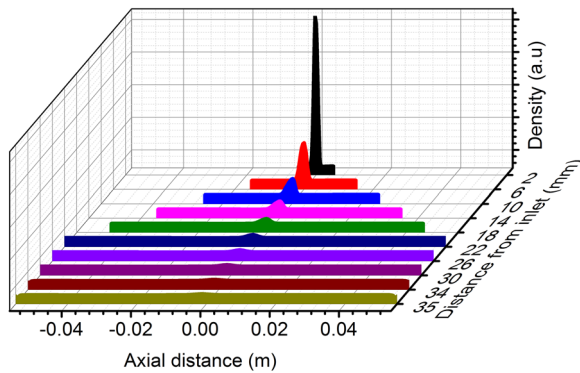
FIG. 4. Lineouts taken along the central part of the *SlitCell* showing the evolution of the gas density profile as it propagates from the inlet to the gas cell section. The profiles are plotted in steps of 4 mm beginning with 2 mm above the inlet (black curve). The density profile initially presents a very strong density spike that decreases very fast as it propagates through the *SlitCell*.

The reasons why we have chosen this kind of geometry for the *SlitCell* are as follows. The gas enters the slit nozzle through a small 0.1 mm diameter inlet, as shown in Fig. 4, and expands continuously inside the slit nozzle as it propagates towards the nozzle outlet. The slit nozzle shape and length ensure that the gas density profile, as it exits the slit nozzle and enters the gas cell, is uniform. The gas fills the gas cell uniformly and exits through two 1.4 mm diameter outlets. Although the density profile initially presents a very strong density spike (see the black profile in Fig. 4) as it enters the gas cell at 20 mm above the inlet, the difference between the density spike and flat profile is around 10%. The gas propagates further to the central axis of the cell part at 35 mm above the inlet and the density spike along the central axis reduces a negligible level of 2% difference. The density spike can be further reduced by increasing the distance between the inlet and gas cell part but in our case it was not feasible due to space restrictions inside the vacuum chamber used for experiments. These simulation results from ANSYS Fluent with helium at pressure of 10 bars show that the combination of the slit nozzle and gas cell forms the proper geometry for the new gas target, the *SlitCell*.

C. Characterization method

The gas density profile of the *SlitCell* has been retrieved using a Mach-Zehnder interferometer. Figure 5 shows the schematics of the interferometer. The interferometer consists of a HeNe laser with a wavelength of 633 nm, 10 mm diameter, two 50/50 beam splitters (BS1, BS2), two mirrors (M1, M2), and a CCD camera connected to a computer. The *SlitCell* is mounted on a motorized linear stage and installed in a vacuum chamber. The laser beam of one interferometer arm passes through the windows of the vacuum chamber and the *SlitCell* lateral windows. Due to this geometrical arrangement, the density measurements are averaged along the direction of propagation of the probe beam. The gas cell has been translated perpendicularly to the laser beam axis to scan the entire length of the gas cell. The translation is made in steps of 8 mm so that the 2 mm region is overlapped in the scanning to insure the continuity between each step.
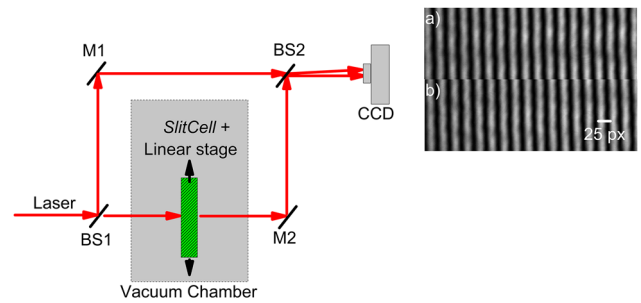

FIG. 5. Schematic drawing of the Mach-Zehnder interferometer with the gas cell placed in one of the arms. Typical interferograms obtained (a) with gas present in the *SlitCell* and (b) without gas (reference). The *SlitCell* is translated along the perpendicular direction relative to the laser beam propagation.

In order to obtain the gas density profile, we recorded two interferograms for each step: one without gas for reference and one with gas for signal. For the measurement, argon gas was chosen due to its high refractive index n = 1.000 281. The gas density can be obtained from the fringe shift of the interferogram by the formula[20] $\rho = \frac{\Delta m \lambda \rho_0}{L(n_{gas}-1)}$, where Δm is the ratio between the fringe shift with gas from the reference and the fringe distance in the reference, λ is the laser wavelength, $\rho_0 = 2.68 \times 10^{19}$ cm^{-3} for argon, L (=3 cm) is the lateral length of medium along the beam propagation, and n_{gas} is the refractive index of the gas at atmospheric pressure with 300-K temperature. The distance between two consecutive fringes in the reference is 25 pixels which corresponds to approximately 0.13 mm spatial resolution. The noise level is about ±1 pixel in fringe shift which corresponds to a density noise of $\pm 8.54 \times 10^{16}$ atoms/cm^3. Since the mechanical vibrations from the environment have been present during the measurements although a stabilized optical table has been used, we have applied a relatively long exposure time of 1.5 s to the camera for averaging the effects of mechanical vibrations. In terms of pixels, the vibration amplitude has been of the order of ±2 pixels, thus any averaged local inhomogeneity below the error level cannot be detected. The gas has been flown continuously in the *SlitCell* to ensure the steady state flow condition during the measurements, and, thus, the long exposure time of the camera has not blurred the fringes due to transient evolution of the gas flow.

D. Comparison between measurements and CFD simulations

The *SlitCell* has been first characterized through fluid dynamics simulations, which have been validated by interferometry measurements. Figure 6 shows the measured density profiles (full line curves) along the central axis of the gas cell (straight line between the two gas outlets in the gas cell part) and CFD simulation results (dashed line) for backing pressures of 10 bars, 16 bars, and 24 bars. The main source of errors is the long exposure time and the pixel-to-pixel noise that leads to a density error about $\pm 1.7 \times 10^{17}$ atoms/cm^3. The measured density profile closely matches the CFD simulations within the range of the experimental errors. There have been small differences of 6.6% in average between measurements and simulations for the backing pressures of 16 bars and 24 bars with 80-mm long *SlitCell*, which may be caused by
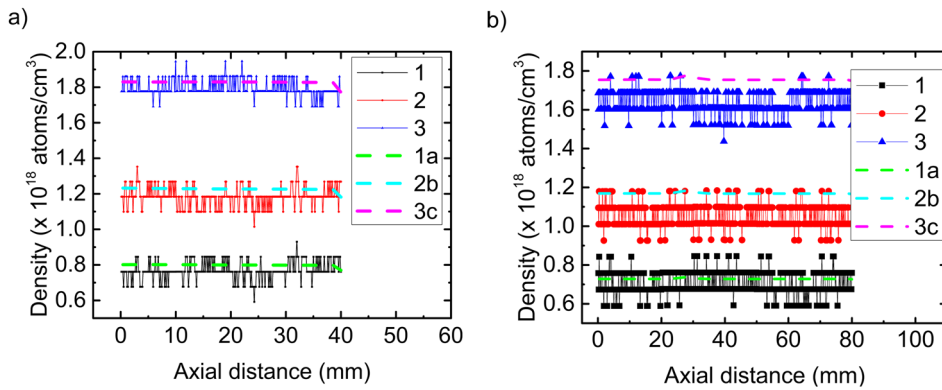
FIG. 6. (a) Gas density profile for the *SlitCell* with 40 mm length and (b) gas density profile for the *SlitCell* with 80 mm length. 1a, 2b, and 3c dashed lines represent the results from simulations with helium at 10 bars, 16 bars, and 24 bars, respectively, and the 1, 2, and 3 full lines represent the results from interferometry with argon at 10 bars, 16 bars, and 24 bars, respectively.

small geometrical differences between the manufactured and simulated *SlitCell*. Also, CFD simulations (not shown here) done using Ar and He could not show any difference in the density profiles that are detectable by our measurement system. In the measurement, the density profiles taken along the central axis of the cell have not presented any density spikes, within experimental error mentioned earlier, at the middle of the gas cell. Thus, we can conclude that our design of *SlitCell* has been validated as a tool for providing a long and uniform gas medium for LWFA.

The *SlitCell*, although simple in design, can be customized to generate more complicated profiles. For instance, the density profiles can be shaped in step-like form as required[21] for staged LWFA[7] by adding several stages similar in design with the *SlitCell*. This kind of customizable *SlitCell* is currently under development and its details will be presented later in a separate publication. Additional simulations (not presented here) showed that the *SlitCell* length can be extended even to several tens of centimeters without affecting the uniformity of the density profile. Consequently, the *SlitCell* is a versatile gas target that could be a useful gas medium for studying various interactions between intense laser pulses and gaseous medium, especially for LWFA with PW lasers.[22,23]

III. CONCLUSIONS

We have presented a novel gas target, called in this work *SlitCell*, designed for LWFA experiments. The new gas target consists of a gas cell that has a gas inlet in the shape of the slit nozzle and generates a very uniform length and density variable density profile. This result, combined with the customizability of density profiles, gives us a versatile apparatus that could improve the present wakefield accelerators and further develop the laser-based accelerators.

ACKNOWLEDGMENTS

[1]T. Tajima and J. M. Dawson, "Laser electron accelerator," Phys. Rev. Lett. **43**, 267–270 (1979).
[2]E. Esarey, C. Schroeder, and W. Leemans, "Physics of laser-driven plasma-based electron accelerators," Rev. Mod. Phys. **81**, 1229–1285 (2009).
[3]W. Lu *et al.*, "Generating multi-GeV electron bunches using single stage laser wakefield acceleration in a 3D nonlinear regime," Phys. Rev. Spec. Top.–Accel. Beams **10**, 061301 (2007).
[4]S. Banerjee *et al.*, "Generation of tunable, 100-800 MeV quasi-monoenergetic electron beams from a laser-wakefield accelerator in the blowout regime," Phys. Plasmas **19**, 56703 (2012).
[5]T. J. Yu *et al.*, "Generation of high-contrast, 30 fs, 1.5 PW laser pulses from chirped-pulse amplification Ti:sapphire laser," Opt. Express **20**, 10807–10815 (2012).
[6]J. H. Sung, S. K. Lee, T. J. Yu, T. M. Jeong, and J. Lee, "0.1 Hz 1.0 PW Ti:sapphire laser," Opt. Lett. **35**, 3021–3023 (2010).
[7]H. T. Kim *et al.*, "Enhancement of electron energy to the multi-GeV regime by a dual-stage laser-wakefield accelerator pumped by petawatt laser pulses," Phys. Rev. Lett. **111**, 165002 (2013).
[8]W. P. Leemans *et al.*, "Multi-GeV electron beams from capillary-discharge-guided subpetawatt laser pulses in the self-trapping regime," Phys. Rev. Lett. **113**, 245002 (2014).
[9]X. Wang *et al.*, "Quasi-monoenergetic laser-plasma acceleration of electrons to 2 GeV," Nat. Commun. **4**, 1988 (2013).
[10]T. Hosokai *et al.*, "Supersonic gas jet target for generation of relativistic electrons with 12TE-50 fs laser pulse," in *Proceedings of EPAC 2002, Paris, France* (EPAC, 2002), pp. 981–983.
[11]R. Jung, J. Osterholz, O. Willi, R. Heathcote, and D. Neely, "Optimization and characterization of supersonic gas jet target for laser-plasma interaction studies," Central Laser Facility Annual Report, 2004, pp. 23–24.
[12]J. P. Couperus *et al.*, "Tomographic characterisation of gas-jet targets for laser wakefield acceleration," Nucl. Instrum. Methods Phys. Res., Sect. A **830**, 504–509 (2016).
[13]K. Schmid and L. Veisz, "Supersonic gas jets for laser-plasma experiments," Rev. Sci. Instrum. **83**, 53304 (2012).
[14]J. Osterhoff *et al.*, "Generation of stable, low-divergence electron beams by laser-wakefield acceleration in a steady-state-flow gas cell," Phys. Rev. Lett. **101**, 85002 (2008).
[15]F. Brandi *et al.*, "Note: Real-time monitoring via second-harmonic interferometry of a flow gas cell for laser wakefield acceleration," Rev. Sci. Instrum. **87**, 86103 (2016).
[16]Fluent, ANSYS Fluent 12.0 User's Guide, Ansys, Inc., Vol. 15317, pp. 1–2498 (2009).
[17]R. Hagmeijer, *Fluid Mechanics I* (Springer, 2014).
[18]P. Kundu and I. Cohen, *Fluid Mechanics* (Academic Press, San Diego, CA, 2004).
[19]J. D. Anderson, *Computational Fluid Dynamics: The Basics with Applications*, McGraw-Hill Series in Mechanical Engineering, McGraw-Hill Series in Aeronautical and Aerospace Engineering, McGraw-Hill International Editions, Mechanical Engineering Series (McGraw-Hill Education, 1995).
[20]S. Semushin and V. Malka, "High density gas jet nozzle design for laser target production," Rev. Sci. Instrum. **72**, 2961 (2001).
[21]A. Pukhov and I. Kostyukov, "Control of laser-wakefield acceleration by the plasma-density profile," Phys. Rev. E **77**, 025401R (2008).
[22]Y. Chu *et al.*, "High-energy large-aperture Ti:sapphire amplifier for 5 PW laser pulses," Opt. Lett. **40**, 5011 (2015).
[23]J. H. Sung *et al.*, "4.2 PW, 20 fs Ti:sapphire laser at 0.1 Hz," Opt. Lett. **42**, 2058 (2017).